Demobase project : numerical simulation for seamless integration of battery pack in light electric vehicle

Martin Petit, Sara Abada, Rémy Mingant, Julien Bernard, Philippe Desprez, Pietro Perlo, Marco Biasiotto, Riccardo Introzzi, Amandine Lecocq, Guy Marlair

HAL Id: ineris-03237715

https://ineris.hal.science/ineris-03237715

Submitted on 26 May 2021

Demobase project: Numerical simulation for seamless integration of battery pack in light electric vehicle

Martin PETIT[1], Sara ABADA[1], Rémy MINGANT[1], Julien BERNARD[1], Philippe DESPREZ[2], Pietro PERLO[3], Marco BIASIOTTO[3], Riccardo INTROZZI[3], Amandine LECOCQ[4], Guy MARLAIR[4]

[1] *IFP Energies Nouvelles, Electrochemistry and Materials Departement, BP3 69390 Solaize (France)*

[2] *SAFT, 111/113 Boulevard Alfred Daney, 33074 Bordeaux (France)*

[3] *I-FEVS, Carignano, 50/1, 10040 La Loggia Torino (Italia)*

[4] *INERIS, Parc Technologique Alata, 60550 Verneuil en Halatte*

Summary

In the scope of DEMOBASE project, numerical simulation is used to design an efficient and safe storage system for a light-weight electric vehicle. Multi-scale modelling is used in order to assess the safety of the battery pack when submitted to thermal and electrical abuse situations. 3 cells generations are to be studied in the project so that development times should be reduced. First study has been carried out on the first generation with the calibration of lumped electrothermal model taking into account thermal runaway. 0D numerical simulation on module behaviour with abuse-tolerant design show the effect of new materials on the module safety.

Keywords: battery, safety, modelling, simulation

1   Introduction

Electrification in automotive application has been part of a wide effort to reduce greenhouse gases emission following policies of major governments in the world and more specifically in the EU. These policies' success will rely on the development of new electric vehicles able to tackle main challenges of first generation EVs being high cost, lack of autonomy and also safety concerns [1]. As a consequence, critical choice needs to be made as soon as the development and prototyping phase.

Modelling can then play a crucial role in order to anticipate and validate the choices made and that is specifically the scope of the DEMOBASE project (DEsign and MOdelling for improved BAttery Safety and Efficiency) aiming at developing an innovating EV concept meeting new market demand. The strategy presented in Figure 1 takes safety into account at every stage of EV design and is fully supported by state-of-theart modelling and experimentation on Li-ion cells and modules. DEMOBASE project is focused on an innovative lightweight vehicle dedicated to passenger transportation in urban conditions. This vehicle is under development at I-FEVS and the battery pack is particularly scrutinized in the scope of this project as 3 battery generations manufactured by SAFT are to be tested. At this stage the developments have been carried out on the first generation of batteries.

In the early stage of the project, system modelling of the vehicle [2] permitted to evaluate the performances of the vehicle and size a fit-for-purpose electric storage system. Then the work was focused on the safety of the storage system module in order to provide design recommendations that help to build a safer battery pack. Modelling thermal runaway has been a hot working subject since the last decade [1] with 0D or 3D thermal models based on thermochemical degradation reactions [3–6] ,such modelling approaches have been applied up to module level [7, 8].. For instance, for studying 16p module Smith et al. [9] represented cells within a module as a temperature network with 5 sub-cells. Kim et al. [3] compared a 3D thermal model with a lumped approach model to study the thermal behaviour of cylindrical cells . This study showed that although lumped approach is not able to tackle localised phenomena such as localized short circuits, they are able to reproduce overall behaviour of the cell. In order to test multiple designs, a simplified lumped thermal remains the preferred approach to allow fast calculation. Thus, in our approach, to model pouch cells we have adopted a lumped thermal behaviour modelling approach implemented in Siemens PLM Software Simcenter Amesim ™.

In this paper, we focus on the 0D modelling of the battery module to test the thermal behaviour of the battery in both normal and abuse conditions.
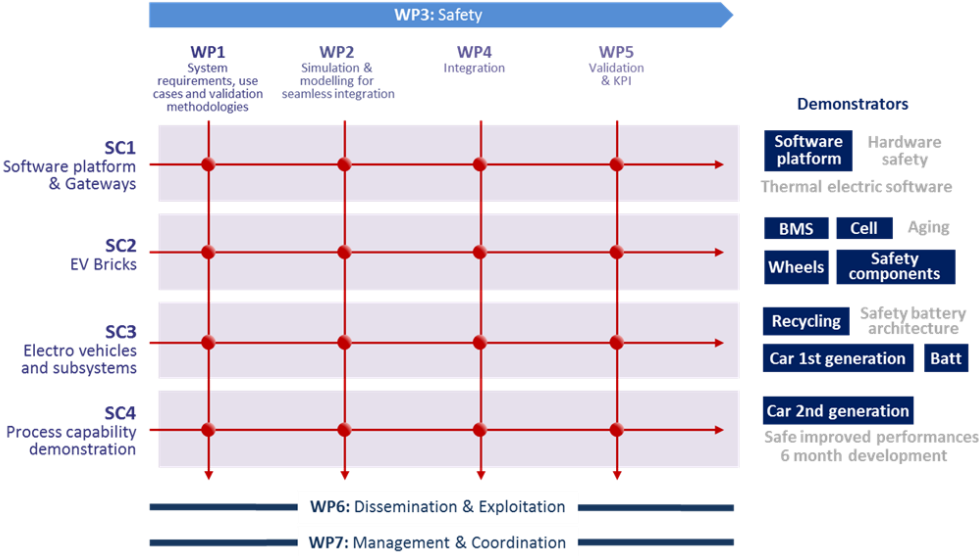

Figure 1: Overall structure of the DEMOBASE project

2   0D safety modelling

In order to assess the safety of the designed module, a 0D modelling approach has been performed. It allows fast computing of thermal behaviour of a large module taking into account heat exchanges between modules technical parts. The basis of this model relies on a thermal runaway model.

2.1   Battery electrothermal model

The battery electrothermal model consists of an empirical electrical equivalent circuit in which a voltage source is used for the open circuit voltage depending on SOC (State Of Charge) and temperature; a high frequency resistor and two RC loops are implemented to model transient phenomena. All the resistors and capacitors depend on SOC and temperature.

This model is able to represent the electrical and thermal behavior of the cell and has been calibrated thanks to dedicated tests performed in IFPEN test benches.

2.2 Thermal runaway modelling

Thermal runaway (TR) is an undesirable event liable to compromise LIBs safety technology which occurs when heat exchange is not sufficient to evacuate heat flow from the cell. The heat accumulation inside the cell progressively increases the cell temperature and activates cascading degradation reactions. The main reactions taken into account in our model are the following [10]:

1. Metastable SEI stabilization
2. Solvent reduction on the negative electrode (SEI formation)
3. Positive electrode decomposition
4. Electrolyte decomposition
5. Self-discharge / short-circuit
6. Venting

The reactions 1 to 5 are all exothermal. Reactions 1 to 4 may release gases which increase the internal pressure of the cell. When the pressure is higher than the critical threshold activating a pressure discharge pre-calibrated relief valve, the venting occurs.

An empirical approach is chosen to describe this phenomenon, where thermochemical reactions are represented by dimensionless figures based on Kim et al [11], Abada et al [1, 6].

The aim of the thermal runaway model is to evaluate the global heat released by the degradation reactions as follows:

$$Q_{abuse} = Q_{SEI} + Q_{ne} + Q_{nb} + Q_{pe} + Q_{ele} + Q_{vent} + Q_{sd} \tag{1}$$

Where the volumetric abuse reactions heat Q_{abuse} is calculated as the sum volumetric heat releases of degradation reactions: Q_{SEI} for the SEI degradation, Q_{ne} for the negative electrode degradation, Q_{pe} for the positive electrode and Q_{ele} from the electrolyte, Q_{sd} from the self-discharge and finally Q_{vent} from venting.

The reaction between the electrolyte and the fluorinated binder is neglected as well as the reaction with lithium metal: this latter reaction plays a bigger role in the case of battery overcharge which is not covered in our study.

For each generation, the reaction rate R_i is evaluated as well as volumetric abuse reaction rates. Reactions 1 to 4 have been described in former papers [6] and we will focus here on new mechanisms added to this model being self-discharge and venting.

2.2.1 Self-discharge reaction

At high temperature, the cell undergoes short-circuit leading to the voltage decrease until 0V due to the self-discharge current, I_{TR} which is expressed as follows:

$$I_{TR} = -3600 \cdot A_{ec} \cdot exp(\frac{-E_{a,ec}}{k_B \cdot T}) \cdot U_{cell} \cdot Q_{cell}$$

In this expression:

- A_{ec} is the frequency factor of the self-discharge reaction [1/s].
- $E_{a,ec}$ is the activation energy of the self-discharge reaction [J].
- k_B is the Boltzmann constant $1.380 \cdot 10^{-23}$ J $\cdot$ K^{-1}
- U_{cell} is the cell voltage [V].
- Q_{cell} is the cell capacity in [Ah].

This current is then added to the input current of the cell to compute electrochemical heat losses during discharge. Moreover, the power released by discharge is calculated and added to the heat flow generated by abuse reaction. It is expressed as follows:

$$Q_{sd} = U_{cell} \cdot I_{TR}$$

This heat loss is then used in equation (1).

2.2.2 Venting

During thermal runaway decomposition reaction, gases are produced leading to pressure increase inside the cell. Once pressure reaches a given threshold (burst pressure) venting occurs leading to a slight temperature decrease and gas emission inside the module. In our approach, each thermal runaway degradation reaction produces a given amount of gas, n_i, whose rate or formation is expressed as follow:

$$\frac{dn_i}{dt} = R_i w_i V_{g_i} \tag{2}$$

In this expression the rate of gas formation of reaction i, $\frac{dn_i}{dt}$ in mol/s is expressed as a function of its reaction rate R_i, w_i the mass of reactant of reaction i and V_{g_i} the amount of gas produced by reaction i per kg of reactant.

As a consequence of gas formation, pressure inside the cell increases. It can be expressed as a function of initial pressure P_0 in Pa, temperature T in K, head space volume V_h in m^3 and y the amount of gases ejected through the vent in mol:

$$P = P_0 + \frac{RT}{V_h}\left(\sum_i n_i - y\right) \tag{3}$$

Once the pressure reaches the burst pressure, venting occurs. This phenomenon has been mathematically described by Coman et al. [5]. In our case, it has been assumed that there was no mass variation during the process. The amount of material released by venting is evaluated thanks to the Mach number expressed once vent is open as a function of internal and ambient pressures and heat capacity ratio of formed gases γ:

$$M = \max\left(\sqrt{\frac{2}{\gamma - 1}\left(\frac{P}{P_{amb}}\right)^{\frac{\gamma-1}{\gamma}}}, 1\right) \tag{4}$$

Based on this number, venting pressure P_{vent}, temperature, T_{vent}, and velocity, V_{vent}, are evaluated according to following set of ,equations (5) to (7):

$$P_{vent} = \frac{P}{\left(1 + \frac{\gamma - 1}{2}M^2\right)^{\frac{\gamma}{\gamma-1}}} \tag{5}$$

$$T_{vent} = \frac{T}{1 + \frac{\gamma - 1}{2}M^2} \tag{6}$$

$$V_{vent} = \frac{\gamma RT}{M_{gas}}M \tag{7}$$

In these equations, M_{gas} is the molar weight of formed gases. As a consequence, it is then possible to evaluate the rate of gas escaping the cell through venting, making use of equation (8):

$$\frac{dy}{dt} = \frac{P_{vent}V_{vent}A_{vent}}{RT} + \frac{dn_{gas}}{dt} \qquad (8)$$

In this expression, n_{gas} is the amount of gases formed by degradation reactions while the burst pressure relief valve is open. Finally, it is possible to evaluate the energy loss due to power drop during venting from equation (9):

$$Q_{vent} = RT\frac{dy}{dt} \qquad (9)$$

This heat loss is used in equation (1).

This electrothermal model integrating thermal runaway thermophysics has been implemented in the battery cell component of Siemens PLM software Simcenter Amesim [TM] [12].

2.2.3 Thermal runaway model calibration

Thermal and thermochemical parameters of the cell have been obtained by data fitting with experimental data. Thermal parameters where indeed deduced from 2 tests:

- Heat, Wait and Search (HWS) steps before thermal runaway onset in ARC experiments: specific heat capacity of tested cell and heat exchange coefficient with surrounding devices
- Constant current charge/discharge cycles: transversal heat conductivity and entropic coefficient as a function of SOC

Thermochemical parameters for the thermal runaway model were obtained thanks to (HWS) test performed in INERIS testing facilities. During this test, temperature, voltage and gas release are measured. These measurements are then compared to model output for calibration.
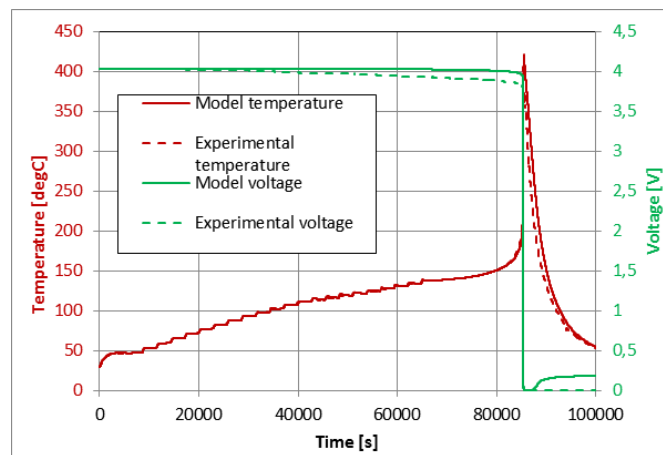

Figure 2: Voltage and temperature evolution versus time: comparison between model prediction and experiment measurements

Figure 2 shows a good agreement between experimental and modelling results regarding voltage and temperature profiles. The model is able to accurately predict the evolution of temperature during the test with a maximum temperature reached being 415°C for both model and experiment. In the same time, voltage drop due to self-discharge is also well predicted at 87 000s. Figure 3 shows that we have been able to calibrate the gas release during the HWS test with a correct amount of gas released 0.57 mol recorded at the corresponding venting event time from the test.

The thermal runaway model is then well calibrated for the first generation of cells, but no validation measurement has been performed yet. These future validations are to be performed in the future tasks of

DEMOBASE project for model use in battery cell and module designing tasks. However, this model will be used by then to offer recommendations of pack design based on this calibration.
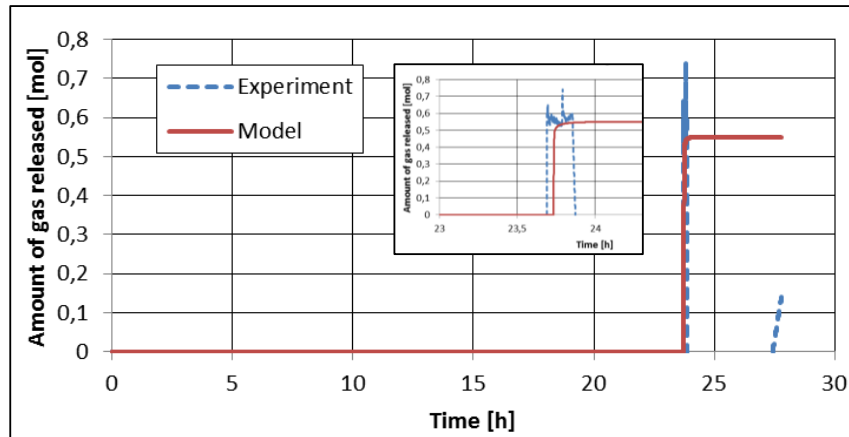

Figure 3: Gas release during HWS test

3 Thermal runaway propagation within a module

The module developed in DEMOBASE project by I-FEVS has n_s =28 cells and n_p =3 parallel branches. In Figure 4, it can be seen that cells are gathered with 3p clusters. Each cell is covered by an aluminium heat sink (cyan). Each cluster is then mechanically constrained by a compression pad (purple) and between each cluster there is a steel firewall (dark grey). A liquid cooling system is implemented below the module.
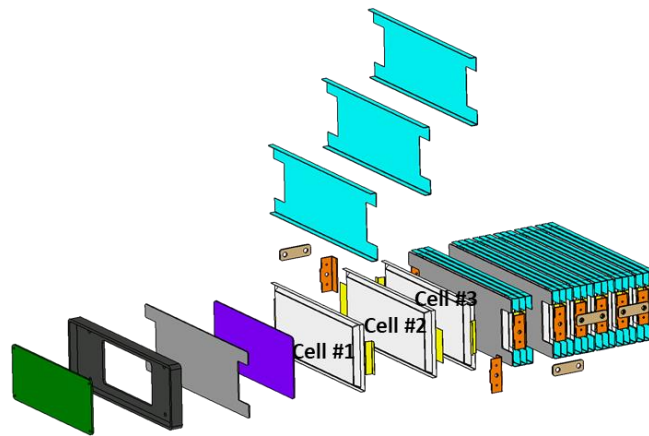

Figure 4: I-FEVS submodule design (3s3p) modelled

3.1 Module thermal modelling

3.1.1 0D model

In order to evaluate module design safety, a Simcenter Amesim model has been developed to represent a 3s3p submodule. In Figure 5, is shown the Simcenter Amesim sketch of this submodule configuration. The model takes into account:

- heat conduction between cells and heat sink.
- heat conduction between cells and busbars.
- heat conduction between cell 1 and compression pad and between compression pad and firewall.

- heat transfer between heat sink and water-cooling system. It is supposed that the water-cooling system operates at 20°C and the heat transfer coefficient is 66.8 W/m²/K.
- heat transfer between busbar and heat sink border with upper lid and environment. It is supposed that external temperature is 20°C and heat transfer coefficient is 1 W/m²/K.

As it is a 0D approach, each component temperature is supposed uniform. Furthermore, metal parts thermal conductivity is higher compared to cell or compression pads. Therefore, interface temperature between metal parts and other elements is supposed to be equal to metal parts temperature.
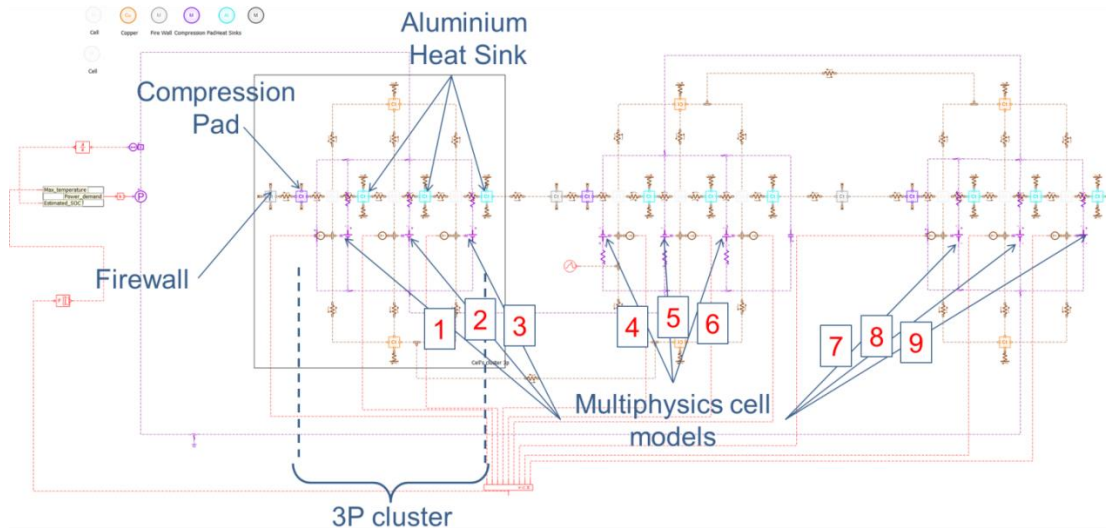

Figure 5: Simcenter Amesim sketch for I-FEVS module simulation

A custom stateflow component is used to provide the module with specific power demands based on sizing scenarios defined by I-FEVS. These power profile scenarios are: a constant power charge at 15kW and different constant power discharge at 15 kW, 25 kW or 40 kW. Battery is cycled between 10 % and 90 % SOC. Continuous cycling is stopped once temperature reaches 150°C and power demand is set to 0W until the end of the simulation.

3.1.2   Normal operating conditions behaviour

Results during a 45 kW scenario simulation are represented in Figure 6 . This simulation shows that there is less than 5°C dispersion between cells temperature and that temperature reaches a maximum value around 35°C. The results of less power demanding scenarios show also the same trend. These simulations validate this first design for normal operating conditions.
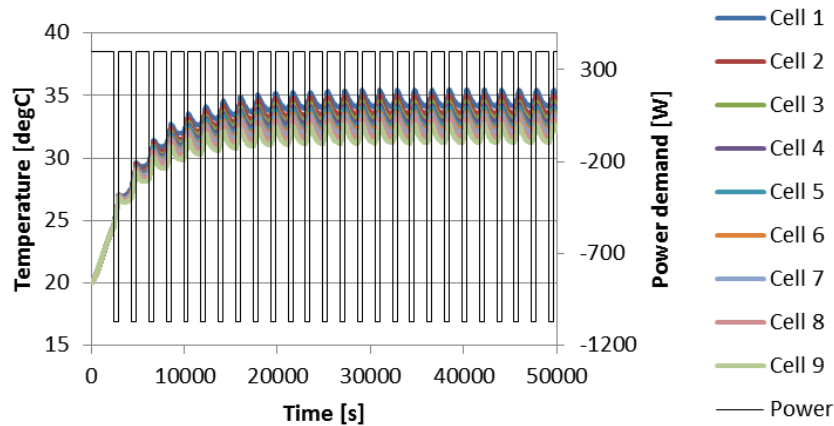

Figure 6: Cells temperatures during max power simulation

3.2 Thermal runaway simulations

Abnormal operating conditions have then been tested to assess the module behaviour when thermal runaway occurs. Several thermal or electrical abuse conditions on operating battery module have been simulated: cooling system failure, overheating of cell 4, short circuit on the middle cluster. Finally, a specific study on firewall material has been performed.

3.2.1 Cooling system failure

To model a cooling system failure, heat transfer at the bottom side of heat sinks is fixed at 0.5 W/m²/K based on I-FEVS specification of module design. In Figure 7, the evolution of the maximum temperature of the submodule is represented for each power scenario presented earlier. It shows that thermal runaway is irreversible when 150°C is reached. If the module is continuously charged and discharged under these scenarios it will go into thermal runaway after 26h of steady state solicitation in the 15 kW scenario and after 20h of steady state solicitation in the 2 other scenarios.
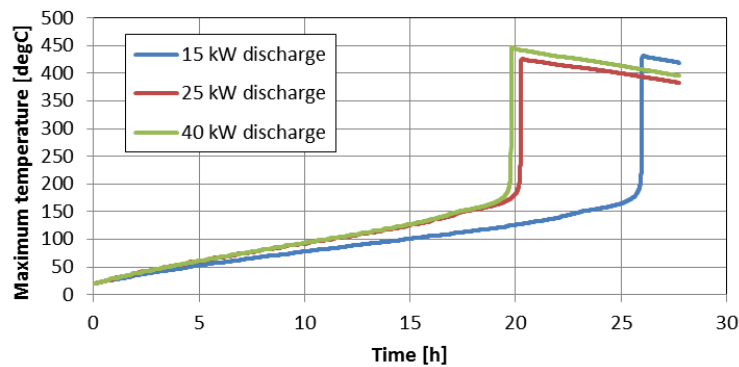

Figure 7: Maximum cell temperatures during simulation with cooling failure

It is to be noted that such solicitation are extreme scenarios and should a cooling failure occur, module operation should stop immediately, as a result of BMS safety function activation in these conditions in such circumstances. It is not expected to wait for more than 20 h before stopping battery operation.

3.2.2 Overheating-induced thermal runaway

When cells are set at rest at 50% SOC, cell 4 is overheated by applying an additional heat flow source to its energy balance. Typically, after 1h rest 1 000 W are injected into cell 4 causing a thermal runaway. In Figure 8, it can be seen that quickly after the initiation of the thermal runaway in cell 4, cells 5 and 6 (from the same cluster) go into thermal runaway.
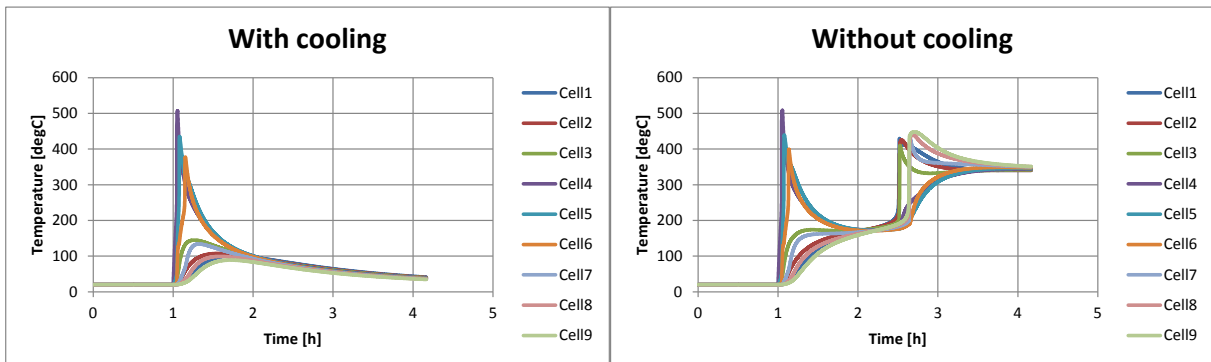

Figure 8: Submodule thermal behaviour following overheating of cell4

The propagation of the thermal runaway to other clusters depends on the state of the cooling system. As showing in Figure 8. In the case of active cooling system (left), heat is sufficiently dissipated and the 2

other clusters are not contaminated. Their temperatures remain below 150°C and all cells temperature decrease to 20°C after several hours.

While in the case of a cooling system failure (right), temperature increases in the other clusters, it reaches 150°C causing thermal runaway of clusters' cells after 1.5h from the initiation event. We can observe in addition a slower decrease of the middle cluster temperature in comparison to the case where the cooling system is active.

These simulations show the effect of liquid cooling system on thermal runaway propagation within a module when a thermal failure occurs. As it is designed, the cooling system is able to avoid module contamination after an initiation event in I-FEV battery system.

3.2.3   Short circuit induced thermal runaway propagation

Another way to initiate thermal runaway is to create an external short circuit on one cluster. To do so, a switch is mounted in parallel with the middle cluster and then closed, resulting in a parallel resistor of 0.1 mΩ. Results are presented in Figure 9. In this simulation the cooling system is switched off. Heat released by the parallel resistor is not taken into account in these simulations.
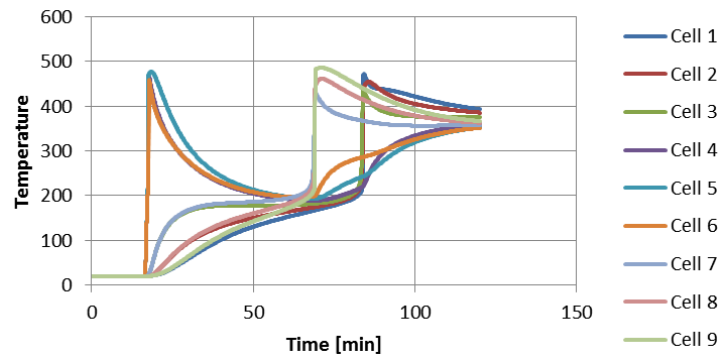

Figure 9: Module thermal behaviour after short circuit on middle cluster

Once the short-circuit is applied, all cells in the middle cluster go into thermal runaway and reach almost 500°C. This causes a temperature increase of neighbour clusters. Cluster 3 (cells 7, 8 and 9) subsequently go into thermal runaway

3.2.4   Firewall design study

In order to improve the module behaviour when the cooling system is not active, some simulations have been carried out where firewall material has been changed. In the initial design, the firewall is made of steel which has a high density and a high specific heat capacity. However, its thermal conductivity is also quite high allowing heat to be conducted from one cluster to another. Two other materials have then been tested to replace steel.

Table 1: Erythritol thermal properties [13]

Property	Value
Solid density	1480 kg/m^3
Solid specific heat	2250 J/kg/K
Solid thermal conductivity	0.733 W/m/K
Melting temperature	117.7°C
Latent heat of solidification	339 800 J/kg
Liquid density	1300 kg/m^3
Liquid specific heat	2610 J/kg/K
Liquid thermal conductivity	0.326 W/m/K

The first one is a thermal insulating material, calcium silicate whose density is 2 900 kg/m^3, its specific heat capacity is 1 030 J/kg/K and its thermal conductivity 0.063 W/m/K. Using such a material may prevent thermal runaway to contaminate other clusters.

The second one is erytrithiol. It is a phase changing material (PCM) whose melting temperature is around 1177°C. Its thermal properties are given in Table 1. Its properties seem also to be matching the applications requirements with a density close to the battery's and relatively high specific heat capacity. Its melting temperature allows high heat absorption just before triggering thermal runaway.
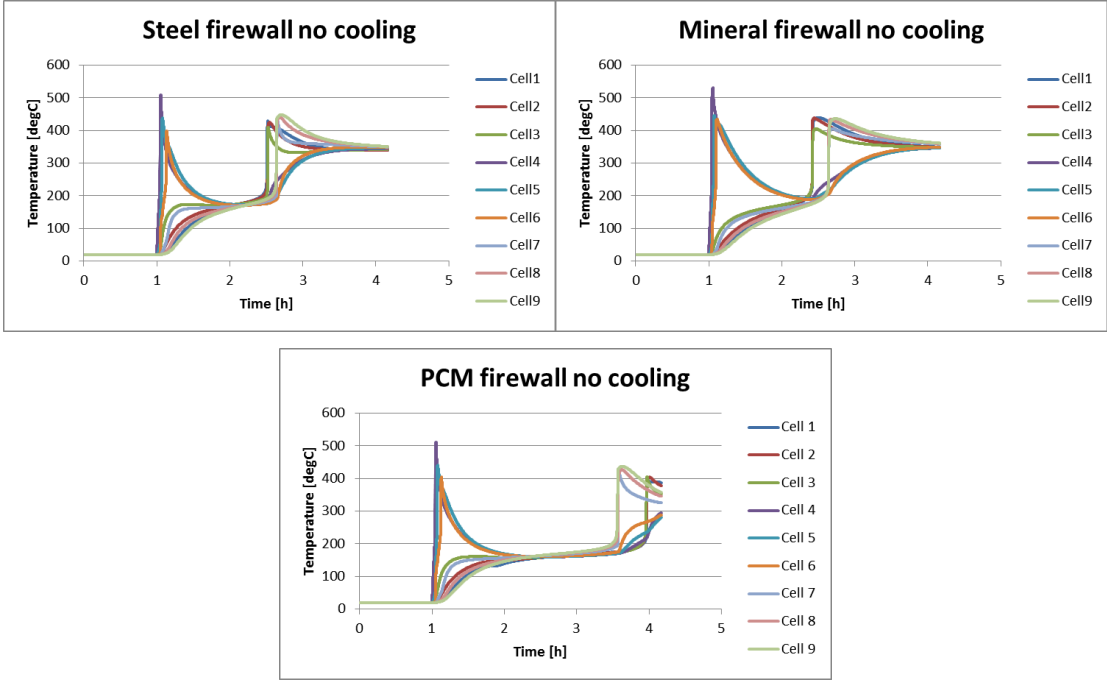

Figure 10: Thermal runaway propagation depending on firewall material

Results from simulations with these new materials after a thermal runaway of cell 4 triggered by overheating is shown in Figure 10. The replacement of steel firewall by a mineral firewall has not changed much the module thermal behaviour. Cluster 1 goes into thermal runaway after 1.5h from initiation while there is some more lag (20 min) before the propagation to the last cluster. Despite the reduced heat conduction between clusters it is not sufficient to improve the safety since there is no heat dissipation to the external environment.

In the case where the steel firewall is replaced by a PCM the time lag before other clusters go into thermal runaway is greater (2.5h after initiation for cluster 3 and cluster 1 goes into thermal runaway 30 min later). In this case, heat is absorbed during phase changing of the PCM. Even though heat is not dissipated outside the system (thermal runaway in other clusters occurs anyway), it is sufficient to slow down thermal runaway propagation. The use of a PCM appears as a good choice to improve safety design.

4   Conclusions and perspectives

In order to develop new battery module designs, a module electrothermal model based on lumped thermal modelling in Simcenter Amesim has been developed. This model comprises a battery cells submodel based on an empirical electrical circuit equivalent modelling and taking into account thermal runaway. The cell model has been calibrated based on normal operating conditions tests as well as abuse tests. Thermal behaviour simulations have been performed on the initial module design from I-FEVS in order to assess the thermal behaviour of the module.

Based on these preliminary results, it can be seen that the module has been well designed with regards to the target application requirements. Cells temperature dispersion remains limited and cells temperature stays below 35°C in most reasonably expectable stressing conditions. Thermal management of the module is efficiently handled, thanks to a water-cooling system that avoids thermal runaway propagation if a cell is overheated or short circuited. If this cooling system device is not active, 20h of continuous cycling are able to provoke module thermal runaway, but if thermal runaway is triggered on one cell or on a cluster, its propagation cannot be prevented without external assistance. Finally, a specific study on firewall material

showed that using PCM can delay thermal runaway propagation up to 2h compared to initial steel based design.

These preliminary results will be validated in the next steps of the project with proper validation data, at cell level for thermal runaway behaviour and at module level for heat transfer modelling. Specific thermal test will then be carried out to allow a precise calibration of thermal parameters of the module elements. Thanks to these preliminary results design recommendations will be given to develop next generation modules. Finally, this seamless process will be applied to the 2 other battery generation produced for the project to design a fit-for-purpose module.

Acknowledgments

References

[1] S. Abada *et al.,* "Safety focused modeling of lithium-ion batteries: A review," *J.Power Sources*, vol. 306, pp. 178–192, 2016.

[2] F. Badin *et al.,* "Energy efficiency evaluation of a Plug-in Hybrid Vehicle under European procedure, Worldwide harmonized procedure and actual use," in *28th International Electric Vehicle Symposium and Exposition (EVS 28): E-Motional Technology for Humans: May 3-6, 2015 KINTEX, Goyang, Korea*, 2015.

[3] G. H. Kim, A. Pesaran, and R. Spotnitz, "A three-dimensional thermal abuse model for lithium-ion cells," *J.Power Sources*, vol. 170, no. 2, pp. 476–489, http://www.sciencedirect.com/science/article/B6TH1-4NHM55R-6/2/558092c27df1f72dcaff8db9b3a88d4c, 2007.

[4] G. Guo *et al.,* "Three-dimensional thermal finite element modeling of lithium-ion battery in thermal abuse application," *J.Power Sources*, vol. 195, no. 8, pp. 2393–2398, 2010.

[5] R. Spotnitz and J. Franklin, "Abuse behavior of high-power, lithium-ion cells," *J.Power Sources*, vol. 113, no. 1, pp. 81–100, http://www.sciencedirect.com/science/article/B6TH1-476KCYW-1/2/a32a1b05cebc0e9651b77fe8631fae40, 2003.

[6] S. Abada *et al.,* "Combined experimental and modeling approaches of the thermal runaway of fresh and aged lithium-ion batteries," *J.Power Sources*, vol. 399, pp. 264–273, 2018.

[7] C. Yang, G.-H. Kim, S. Santhanagopalan, and A. Pesaran, "Multi-Physics Modeling of Thermal Runaway Propagation in a Li-Ion Battery Module," *Meeting Abstracts*, vol. MA2014-01, no. 1, p. 147, 2014.

[8] R. M. Spotnitz, J. Weaver, G. Yeduvaka, D. H. Doughty, and E. P. Roth, "Simulation of abuse tolerance of lithium-ion battery packs," *J.Power Sources*, vol. 163, no. 2, pp. 1080–1086, http://www.sciencedirect.com/science/article/B6TH1-4MCW9T7-2/2/42a7916da78cd9a9bd5e3a5f052a71cf, 2007.

[9] K. Smith, G.-H. Kim, E. Darcy, and A. Pesaran, "Thermal/electrical modeling for abuse-tolerant design of lithium ion modules," *Int. J. Energy Res.*, vol. 34, no. 2, pp. 204–215, 2010.

[10] Detlef Hoffmann, Martin Petit, Guy Marlair, Sara Abada, and Cao-Yang Wang, "Chapter 10. Safety of Lithium Batteries,"

[11] G.-H. Kim, A. Pesaran, and R. Spotnitz, "A three-dimensional thermal abuse model for lithium-ion cells," *J.Power Sources*, vol. 170, no. 2, pp. 476–489, http://www.sciencedirect.com/science/article/pii/S0378775307007082, 2007.

[12] Siemens PLM software, Ed., "Simcenter Amesim: Electric Storage Library 16," User's Guide, 2014.

[13] J. Pereira da Cunha and P. Eames, "Thermal energy storage for low and medium temperature applications using phase change materials – A review," *Applied Energy*, vol. 177, pp. 227–238, 2016.

Authors

Martin PETIT graduated from Ecole des Mines of Nancy in 2007 and obtained his PhD in chemical engineering of INPL in 2011. He joined IFPEN battery modelling team as an electrochemical engineer in 2012 and has contributed to the development of electrical storage systems models for system simulation in automotive applications. Since 2013, Martin is involved in activities around Li-ion batteries safety modelling.

Sara ABADA graduated a Ph.D. in Electrochemistry in 2016 from Sorbonne University after a Master degree of Process Engineering in 2013. After one year of research engineer position at CEA in charge of battery safety modelling, she joined IFPEN in 2018 as a researcher on electrochemical systems in Electrochemistry and Materials department. Currently, she is working on battery model developments for electric vehicles with focus on safety issues.

Julien BERNARD graduated a Ph.D. in Electrochemistry in 2005 after an Engineering degree of ENSEEG (Ecole Nationale Supérieure d'Electrochimie et d'Electrométallurgie de Grenoble, 2002). After a postdoctoral position, in charge with electrochemical processes, joined IFPEN Energies nouvelles in 2007 as research engineer in Electrochemistry and Materials department, and batterie project leader since 2009 for the transportation business unit.

Philippe DESPREZ graduated from ENSIC of Nancy in 1991 and obtained his PhD in Process engineering of INPL in 1997. He joined SAFT in 1999 as Research Engineer then Group Manager in Battery Management and Modelling fields. He has contributed to evolving the use of CAE in Saft solutions into a highly valuable tool applied from cell design to battery design and management. Since 2018, Philippe is involved in Saft Solid State Program as Simulation Expert. Philippe is DEMOBASE project coordinator

Pietro PERLO achieved the Laurea Degree in General Physics at the University of Torino in 1980. In 1981 he was employed at Centro Ricerche Fiat continuing the collaboration with the University as contract professor for 15 years. He authored over 150 technical and scientific publications. In 2011 he founded "Interactive Fully Electrical Vehicles" I-FEVS. In 2016 he has been appointed contract professor at "MIPT" the Moscow Institute of Physics and Technology. In 2018 he received the MIT certificated on Blockchain Technologies.

Guy MARLAIR is a graduate engineer from *Mines de Douai* (now called IMT), France. He also is holder of post-doctoral degree *HDR* which is France opens door to full professorship at University level and allows PhD fellow supervision. He is currently working at INERIS as a senior research scientist and technical advisor in the Accidental Risk Division of the institute. His current research topics are globally bound to energy transition and bio-economy and encompass essentially safety of energy storage, promotion of safe e-mobility, safety issues pertaining to sustainable advanced and intensified biorefining, among which the use of ionic liquids and biomass residues. Since April 2009, Guy is also acting as the chairman of IEC TC120 dedicated to grid integrated energy storage.